Electronic Supplementary Material (ESI) for Inorganic Chemistry Frontiers.

Supporting Information

In Situ Growth of S-Incorporated CoNiFe(oxy)hydroxides Nanoarrays as Efficient Multifunctional Electrocatalysts

Caihong Fang*, Deliang Zhang, Xin Wang, Ran Li

College of Chemistry and Materials Science, Center for Nano Science and Technology, Key Laboratory of Electrochemical Clean Energy of Anhui Higher Education Institutes, Anhui Normal University, Wuhu, 241000, China

AUTHOR INFORMATION

Corresponding Author

*E-mail: chfang@mail.ahnu.ed.cn;

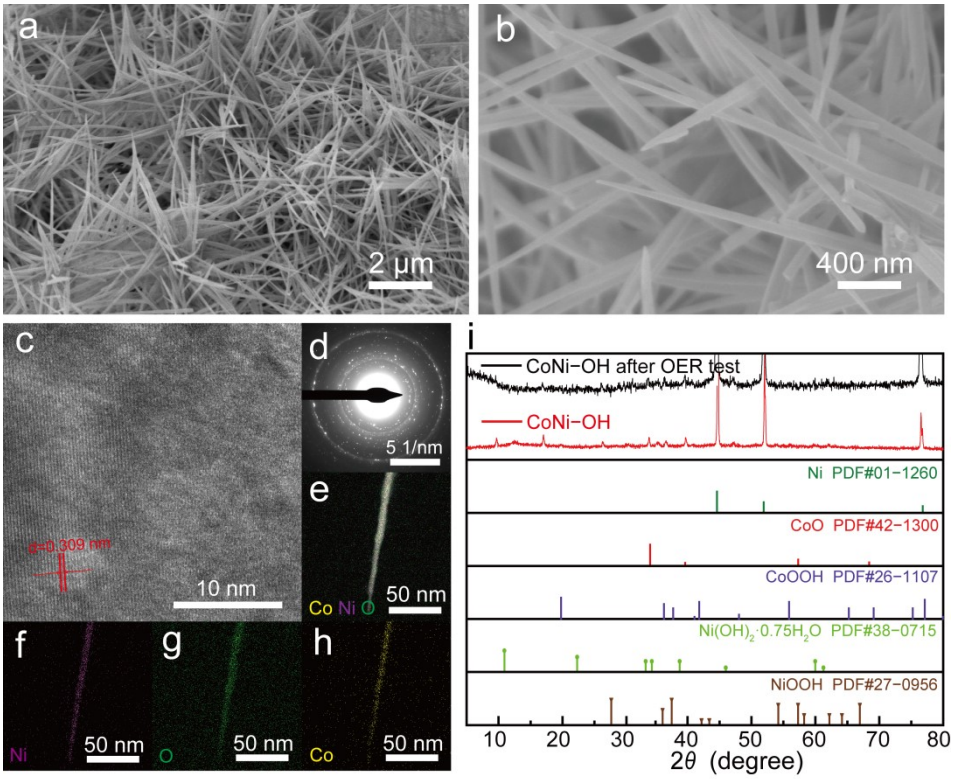

Fig. S1. (a,b) SEM images at different magnifications, (c) HRTEM image,(d) SAED patterns, (e−h) elemental mappings, (i) XRD patterns of the of CoNi−OH nanostructures.

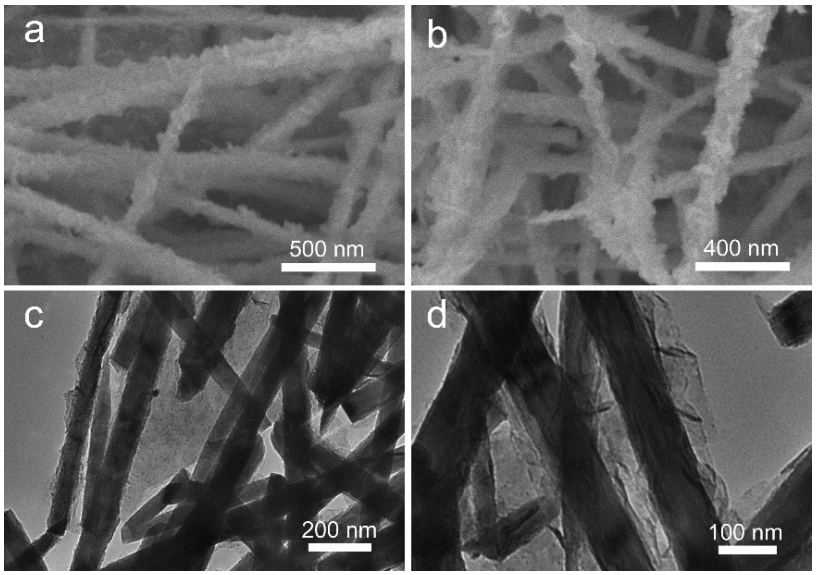

Fig. S2 (a−b) SEM and (c−d) TEM images of CoNiFeS−OH at different magnifications.

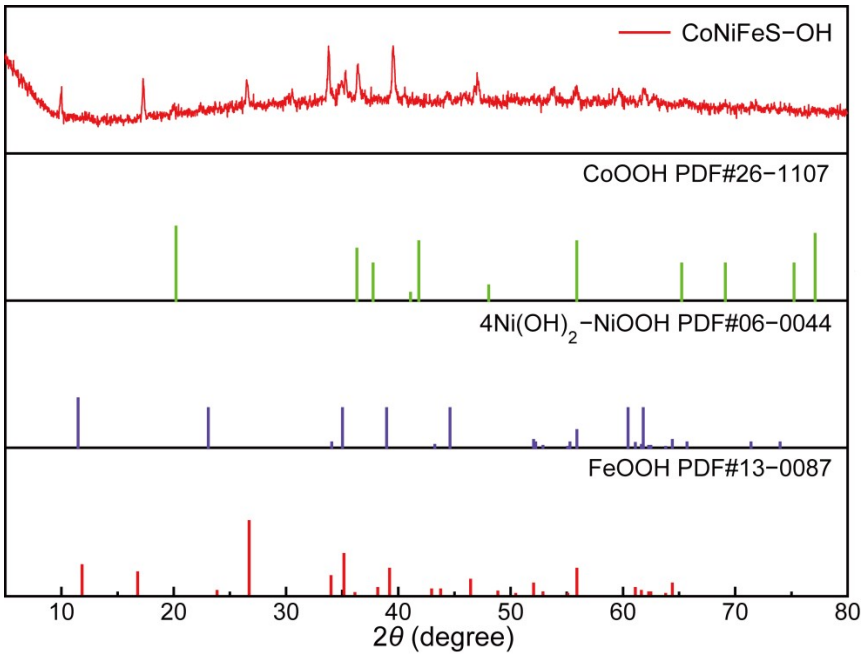

Fig. S3 XRD patterns of CoNiFeS−OH.

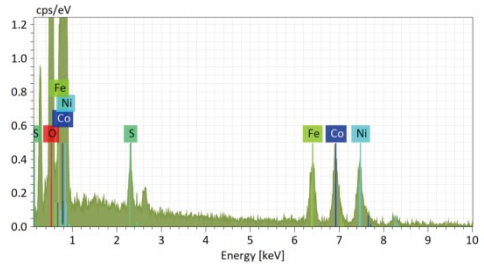

Element	Weight (%)	Atomic (%)
O	36.05	72.55
Fe	11.69	6.74
Co	21.96	12
Ni	14.88	8.16
S	0.54	0.54
Total	100	

Fig. S4 EDS spectra and the corresponding elemental compositions of CoNiFeS−OH.

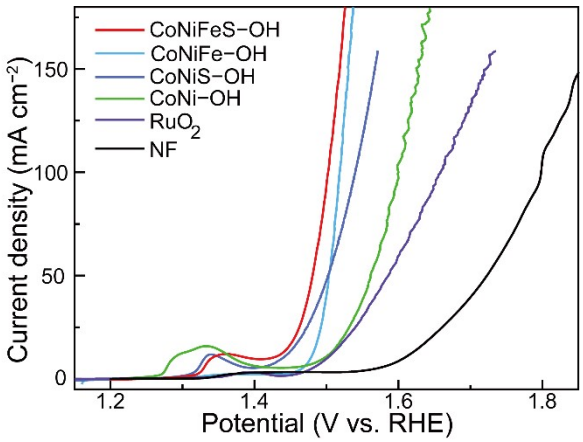

Fig. S5 LSV curves for the OER of CoNiFeS−OH, CoNi−OH, CoNiFe−OH, CoNiS−OH, RuO_2, and NF in 1.0 M KOH at a scan rate of 0.5 mV s^{-1}.

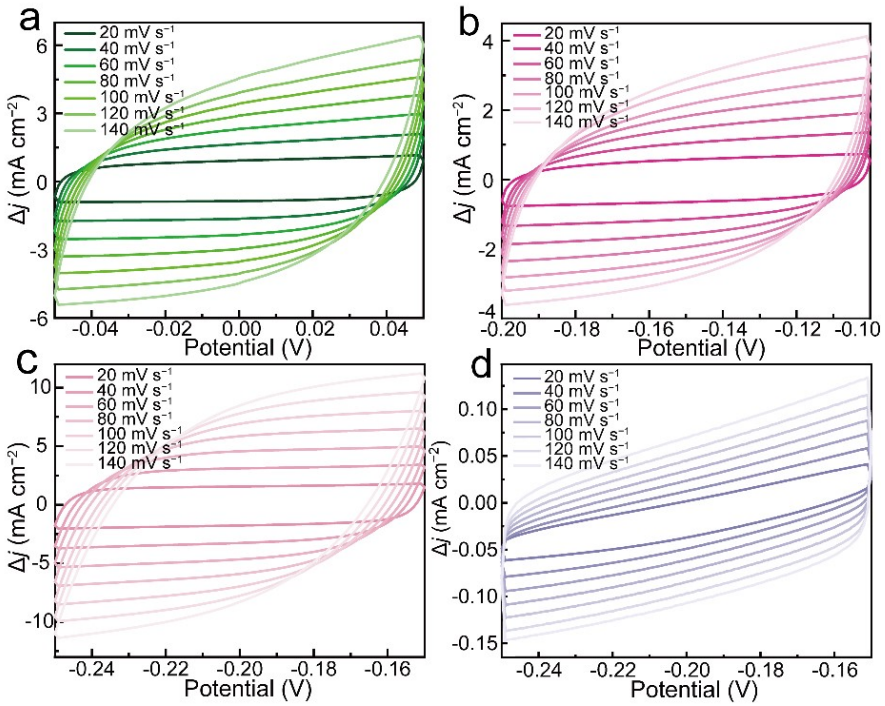

Fig. S6 CV curves for OER measured in KOH (1.0 M) at various scan rates of 20, 40, 60, 80, 100,120 and 140 mV s^{-1}: (a) CoNiFeS−OH, (b) CoNi−OH, (c) RuO_2, and (d) NF, respectively.

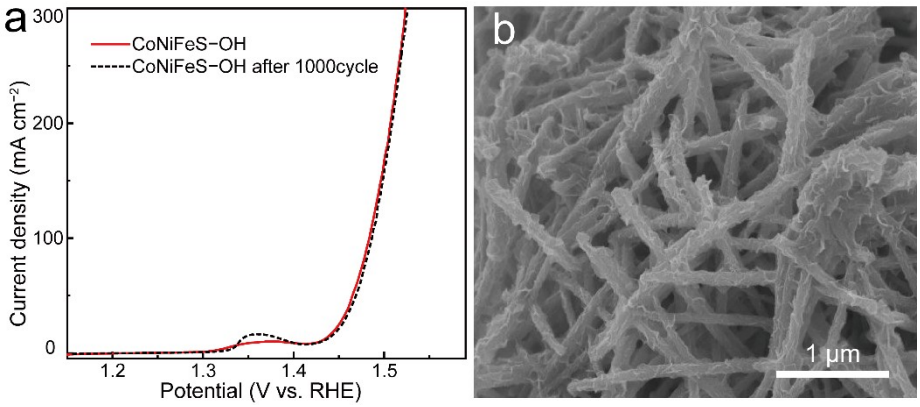

Fig. S7 (a) The polarization curve LSV for OER before and after 1000 CV test of CoNiFeS−OH. (b) SEM of CoNiFeS−OH after 1000 CV in 1M KOH (1.0 M).

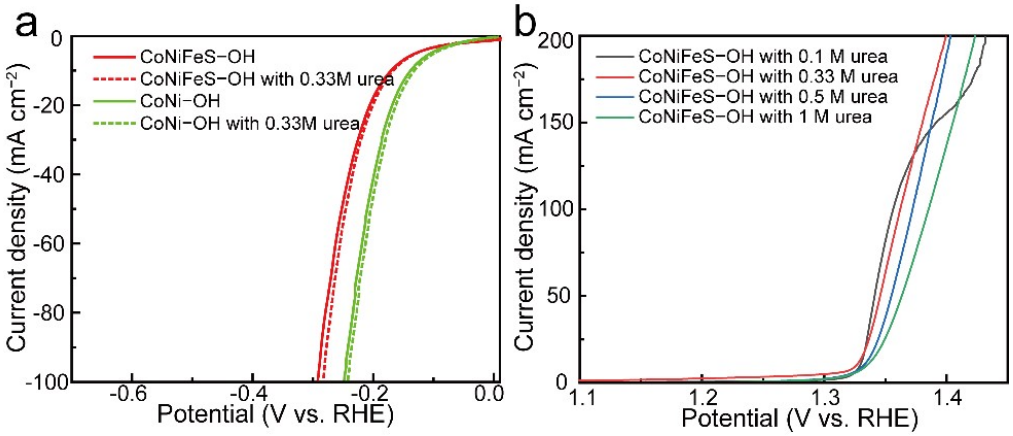

Fig. S8 (a) LSV curves for the HER of CoNiFeS−OH and CoNi−OH in KOH (1.0 M) and in KOH (1.0 M) with urea (0.33 M) at a scan rate of 5 mV s^{-1}. (b) LSV curves for the UOR of CoNiFeS−OH in different urea concentrations at a scan rate of 1 mV s^{-1}.

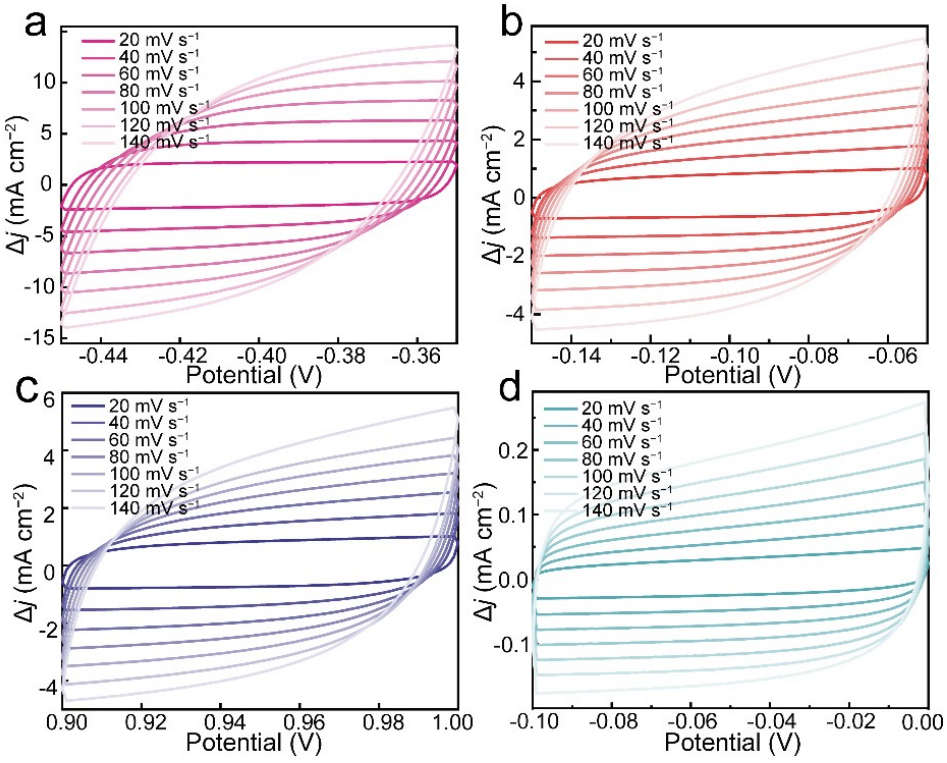

Fig. S9 CV curves for UOR in KOH (1.0 M) with urea (0.33 M) at scan rate of 20, 40, 60, 80, 100, 120 and 140 mV s^{-1}: (a) CoNiFeS−OH, (b) CoNi−OH, (c) RuO_2, (d) NF.

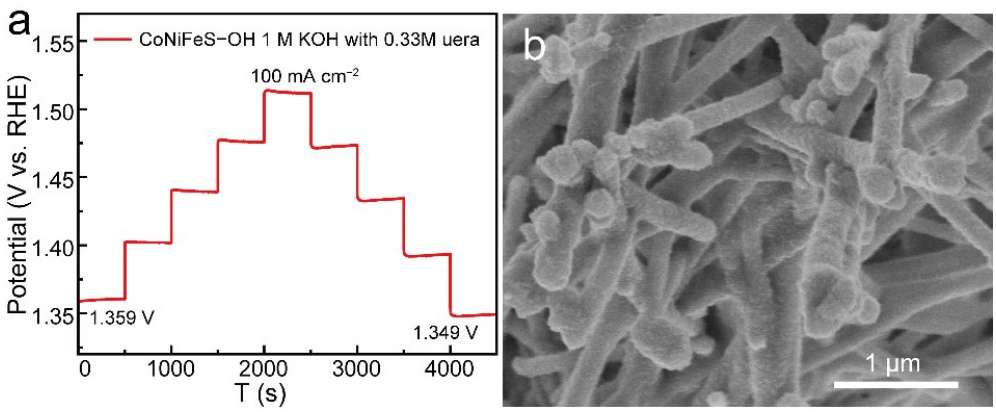

Fig. S10 (a) Multi-step chronopotentiometric curve of CoNiFeS−OH from 20 to 100 mA cm^{-2} in KOH (1.0 M) with urea (0.33 M). (b) SEM of CoNiFeS−OH after 1000 CV in KOH (1.0 M) with urea (0.33 M).

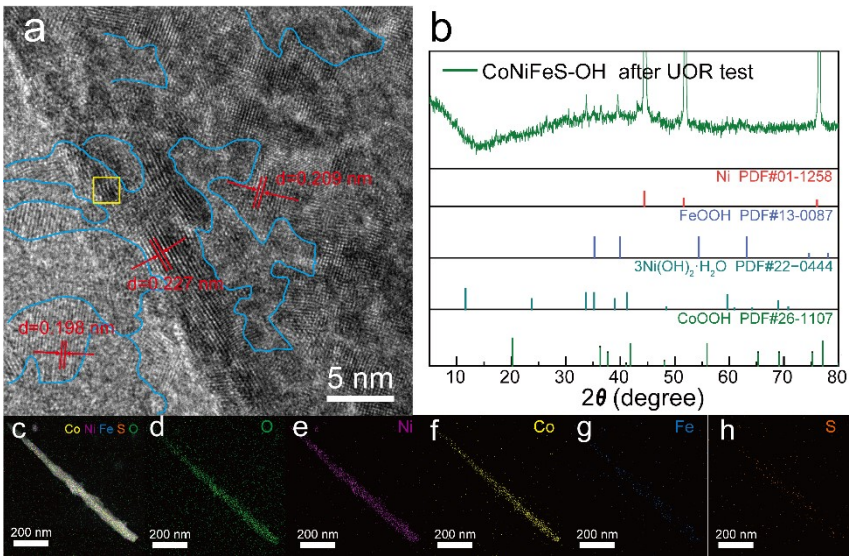

Fig. S11 Characterizations of CoNiFeS−OH catalysts after UOR stability test. (a,b) HRTEM image and XRD patterns, (c−h) elemental mapping of immerged, O, Ni, Co, Fe, and S, respectively.

Table S1 Overpotential of CoNiFeS−OH, CoNi−OH, RuO_2, and NF toward OER at η_{10}, η_{20}, η_{50}, and η_{100} in KOH (1.0 M).

	10 mA cm^{-2} (mV)	20 mA cm^{-2} (mV)	50 mA cm^{-2} (mV)	100 mA cm^{-2} (mV)
CoNiFeS−OH	192	226	251	272
CoNi−OH	260	290	330	370
RuO_2	271	298	355	428
NF	377	415	493	568

Table S2 Comparison for OER properties of CoNiFeS−OH with other non-noble metal based electrocatalysts in KOH (1.0 M).

Catalysts	Substrate	Electrolyte Conc. (KOH)	Current density (mA cm^{-2})	Overpotential (mV)	Ref.
Fe−CoNi−OH	Nickel foam	1M	10	210	1
NiFeCr LDH	Nickel foam	1M	10	225	2
Fe−MOFs@Ni-MOFs@NiFe−LDH	Nickel foam	1M	10	275	3
Fe−Co−αMOF	Nickel foam	1M	10	249	4
CoFeV LDH	Nickel foam	1M	10	242	5
Fe−$Ni(OH)_2$	Nickel foam	1M	10	235	6
$NiCo_2S_4$/FeOOH	Nickel foam	1M	10	~200	7
NiCo−LDH@FeOOH	Carbon papers	1M	10	224	8
NiFePS	Nickel foam	1M	10	242	9
FeCoNiPB/ $(FeCoNi)_3O_{4-x}$	copper foil	1M	10	229	10
CoNiFeS−OH	Nickel foam	1M	10	192	This work

Table S3 Potential of CoNiFeS−OH, CoNi−OH, RuO_2, and NF toward UOR at η_{10}, η_{20}, η_{50}, and η_{100} in KOH (1.0 M) with urea (0.33 M).

	10 mA cm^{-2}(V)	20 mA cm^{-2}(V)	50 mA cm^{-2}(V)	100 mA cm^{-2}(V)
CoNiFeS−OH	1.329	1.338	1.354	1.373
CoNi−OH	1.316	1.333	1.366	1.425
RuO_2	1.388	1.423	1.549	1.645
NF	1.360	1.390	/	/

Table S4 Comparison for UOR properties of CoNiFeS−OH with other non-noble metal based electrocatalysts in KOH (1.0 M) with urea.

Catalysts	substrate	Urea concentration (M)	Current density (mA cm^{-2})	Voltage (V vs RHE)	Ref.
MoS_2/Ni_3S_2	Nickel foam	0.33	20	1.45	11
NiMo alloy	Nickel foam	0.1	10	1.48	12
$NiCo_2S_4$	Carbon cloth	0.33	10	1.45	13
NiMoS	Carbon cloth	0.5	10	1.59	14
$NiCo_2S_4$	Carbon cloth	0.33	10	1.45	15
NiCo LDH	Nickel foam	0.33	10	1.353	16
$FeNi_3−MoO_2$	Nickel foam	0.5	10	1.29	17
Ni@C−250	CP	0.5	10	1.35	18
V−Ni_3N/NF	Nickel foam	0.5	10	1.361	19
NiS/MoS_2	Carbon cloth	0.4	100	1.43	20
CoNiFeS−OH	Nickel foam	0.33	10	1.329	This work

Table S5 Comparison for uera electrolysis efficiency of CoNiFeS−OH//CoNiFeS−OH with other non-noble metal based electrocatalysts in KOH (1.0 M) with urea.

Catalysts	Urea concentration (M)	*j* (mA cm^{-2})	Cell voltage (V)	Ref.
NiFeCo LDH/NF	0.33	10	1.49	21
$NiCo_2S_4$NS/CC	0.5	10	1.49	13
Ni_3S_2-NiS/NF	0.5	50	1.54	22
NC-FNCP	0.5	10	1.52	23
Ni–Co_9S_8/CC	0.33	10	1.52	24
NiMoS/CC	0.5	10	1.59	14
$NiCo_2S_4$/CC	0.33	10	1.45	15
P–NiCoZn LDH/NF	0.5	10	1.479	25
NF/PPy700Ni_3S_2–8–Ar	0.33	10	1.47	26
$(Ni_{0.25}Fe_{0.7}5)_3S_2$/NF	0.33	10	1.49	27
CoNiFeS−OH/NF	0.33	10	1.46	This work

References

(1) Huang, C. Q.; Zhong, Y. H.; Chen, J. X.; Li, J.; Zhang, W.; Zhou, J. Q.; Zhang, Y. L.; Yu, L.; Yu, Y. Fe induced nanostructure reorganization and electronic structure modulation over CoNi (oxy)hydroxide nanorod arrays for boosting oxygen evolution reaction. *Chem. Eng. J.* **2021**, *403*, 126304.

(2) Yang, Y.; Dang, L. N.; Shearer, M. J.; Sheng, H. Y.; Li, W. J.; Chen, J.; Xiao, P.; Zhang, Y. h.; Hamers, R. J.; Jin, S. Highly Active Trimetallic NiFeCr Layered Double Hydroxide Electrocatalysts for Oxygen Evolution Reaction. *Adv. Energy Mater.* **2018**, *8*, 1703189.

(3) Liu, M.; Kong, L. J.; Wang, X. M.; He, J.; Bu, X. H. Engineering Bimetal

Synergistic Electrocatalysts Based on Metal-Organic Frameworks for Efficient Oxygen Evolution. *Small* **2019**, *15*, 1903410.

(4) Liu, C.; Wang, J.; Wan, J. J.; Cheng, Y.; Huang, R.; Zhang, C. Q.; Hu, W. L.; Wei, G. F.; Yu, C. Z. Amorphous Metal–Organic Framework–Dominated Nanocomposites with Both Compositional and Structural Heterogeneity for Oxygen Evolution. *Angew. Chem., Int. Ed.* **2020**, *59*, 3630−3637.

(5) Hu, Y. M.; Wang, Z. L.; Liu, W. J.; Xu, L.; Guan, M. L.; Huang, Y. P.; Zhao, Y.; Bao, J.; Li, H. M. Novel Cobalt–Iron–Vanadium Layered Double Hydroxide Nanosheet Arrays for Superior Water Oxidation Performance. *ACS Sustainable Chem. Eng.* **2019**, *7*, 16828−16834.

(6) Liu, J. L.; Zheng, Y.; Wang, Z. Y.; Lu, Z. G.; Vasileff, A.; Qiao, S. Z. Free-standing single-crystalline NiFe-hydroxide nanoflake arrays: a self-activated and robust electrocatalyst for oxygen evolution. *Chem. Commun.* **2018**, *54*, 463−466.

(7) Li, X.; Kou, Z. K.; Xi, S. B.; Zang, W. J.; Yang, T.; Zhang, L.; Wang, J. Porous $NiCo_2S_4$/FeOOH nanowire arrays with rich sulfide/hydroxide interfaces enable high OER activity. *Nano Energy* **2020**, *78*, 105230.

(8) Han, X. T.; Niu, Y. Y.; Yu, C.; Liu, Z. B.; Huang, H. W.; Huang, H. L.; Li, S. F.; Guo, W.; Tan, X. Y.; Qiu, J. S. Ultrafast construction of interfacial sites by wet chemical etching to enhance electrocatalytic oxygen evolution. *Nano Energy* **2020**, *69*, 104367.

(9) Jeung, Y.; Roh, H.; Yong, K. Co-anion exchange prepared 2D structure Ni(Co,Fe)PS for efficient overall water electrolysis. *Appl. Surf. Sci.* **2022**, *576*, 151720.

(10) Wei, R.; Zhang, K. S.; Zhao, P. j.; An, Y. P.; Tang, C.; Chen, C.; Li, X. M.; Ma, X. L.; Ma, Y. F.; Hao, X. G. Defect-rich FeCoNiPB/$(FeCoNi)_3O_{4-x}$ high-entropy composite nanoparticles for oxygen evolution reaction: Impact of surface activation. *Appl. Surf. Sci.* **2021**, *549*, 149327.

(11) Li, F.; Chen, J. X.; Zhang, D. F.; Fu, W. F.; Chen, Y.; Wen, Z. H.; Lv, X. J. Heteroporous MoS_2/Ni_3S_2 towards superior electrocatalytic overall urea splitting. *Chem. Commun.* **2018**, *54*, 5181−5184.

(12) Zhang, J. Y.; He, T.; Wang, M. D.; Qi, R. J.; Yan, Y.; Dong, Z. H.; Liu, H. F.; Wang, H. M.; Xia, B. Y. Energy-saving hydrogen production coupling urea oxidation over a bifunctional nickel-molybdenum nanotube array. *Nano Energy* **2019**, *60*, 894−902.

(13) Zhu, W. X.; Ren, M. R.; Hu, N.; Zhang, W. T.; Luo, Z. T.; Wang, R.; Wang, J.; Huang, L. J.; Suo, Y. R.; Wang, J. L. Traditional $NiCo_2S_4$ Phase with Porous Nanosheets Array Topology on Carbon Cloth: A Flexible, Versatile and Fabulous Electrocatalyst for Overall Water and Urea Electrolysis. *ACS Sustainable Chem. Eng.* **2018**, *6*, 5011−5020.

(14) Wang, X. X.; Wang, J. M.; Sun, X. P.; Wei, S.; Cui, L.; Yang, W. R.; Liu, J. Q. Hierarchical coral-like NiMoS nanohybrids as highly efficient bifunctional electrocatalysts for overall urea electrolysis. *Nano Res.* **2017**, *11*, 988−996.

(15) Song, W. J.; Xu, M. Z.; Teng, X.; Niu, Y. L.; Gong, S. Q.; Liu, X.; He, X. M.; Chen, Z. F. Construction of self-supporting, hierarchically structured caterpillar-like $NiCo_2S_4$ arrays as an efficient trifunctional electrocatalyst for water and urea electrolysis. *Nanoscale* **2021**, *13*, 1680−1688.

(16) Yan, X. D.; Hu, Q. T.; Liu, J. Y.; Zhang, W. D.; Gu, Z. G. Ultrafine-grained NiCo layered double hydroxide nanosheets with abundant active edge sites for highly enhanced electro-oxidation of urea. *Electrochim. Acta* **2021**, *368*, 137648.

(17) Xu, Q. L.; Yu, T. Q.; Chen, J. L.; Qian, G. F.; Song, H. N.; Luo, L.; Chen, Y. L.; Liu, T. Y.; Wang, Y. Z.; Yin, S. B. Coupling Interface Constructions of $FeNi_3$-MoO_2 Heterostructures for Efficient Urea Oxidation and Hydrogen Evolution Reaction. *ACS Appl. Mater. Interfaces* **2021**, *13*, 16355−16363.

(18) Wang, J. M.; Zhao, Z.; Shen, C.; Liu, H. P.; Pang, X. Y.; Gao, M. Q.; Mu, J.;

Cao, F.; Li, G. Q. Ni/NiO heterostructures encapsulated in oxygen-doped graphene as multifunctional electrocatalysts for the HER, UOR and HMF oxidation reaction. *Catal. Sci. Technol.* **2021**, *11*, 2480−2490.

(19) Li, R. Q.; Liu, Q.; Zhou, Y. N.; Lu, M. J.; Hou, J. L.; Qu, K. G.; Zhu, Y. C.; Fontaine, O. 3D self-supported porous vanadium-doped nickel nitride nanosheet arrays as efficient bifunctional electrocatalysts for urea electrolysis. *J. Mater. Chem. A* **2021**, *9*, 4159−4166.

(20) Zheng, Y.; Tang, P. H.; Xu, X. X.; Sang, X. G. POM derived UOR and HER bifunctional NiS/MoS_2 composite for overall water splitting. *J. Solid State Chem.* **2020**, *292*, 121644.

(21) Babar, P.; Lokhande, A.; Karade, V.; Pawar, B.; Gang, M. G.; Pawar, S.; Kim, J. H. Bifunctional 2D Electrocatalysts of Transition Metal Hydroxide Nanosheet Arrays for Water Splitting and Urea Electrolysis. *ACS Sustainable Chem. Eng.* **2019**, *7*, 10035−10043.

(22) Zhao, Q. Q.; Meng, C.; Kong, D. Q.; Wang, Y. M.; Hu, H.; Chen, X. M.; Han, Y.; Chen, X. D.; Zhou, Y.; Lin, M. C.; Wu, M. B. In Situ Construction of Nickel Sulfide Nano-Heterostructures for Highly Efficient Overall Urea Electrolysis. *ACS Sustainable Chem. Eng.* **2021**, *9*, 15582−15590.

(23) Zhang, J.; Huang, S. S.; Ning, P.; Xin, P. J.; Chen, Z. W.; Wang, Q.; Uvdal, K.; Hu, Z. J. Nested hollow architectures of nitrogen-doped carbon-decorated Fe, Co, Ni-based phosphides for boosting water and urea electrolysis. *Nano Res.* **2021**, *15*, 1916−1925.

(24) Hao, P.; Zhu, W. Q.; Li, L. Y.; Tian, J.; Xie, J. F.; Lei, F. C.; Cui, G. W.; Zhang, Y. Q.; Tang, B. Nickel incorporated Co_9S_8 nanosheet arrays on carbon cloth boosting overall urea electrolysis. *Electrochim. Acta* **2020**, *338*, 135883.

(25) Yang, Z. X.; Zhang, Y. Q.; Feng, C. Q.; Wu, H. M.; Ding, Y.; Mei, H. P doped NiCoZn LDH growth on nickel foam as an highly efficient bifunctional

electrocatalyst for Overall Urea-Water Electrolysis. *Int. J. Hydrogen Energy* **2021**, *46*, 25321−25331.

(26) Zhang, Y. X.; Qiu, Y. F.; Wang, Y. P.; Li, B.; Zhang, Y. Y.; Ma, Z.; Liu, S. Q. Coaxial Ni-S@N-Doped Carbon Nanofibers Derived Hierarchical Electrodes for Efficient H_2 Production via Urea Electrolysis. *ACS Appl. Mater. Interfaces* **2021**, *13*, 3937−3948.

(27) Liu, C.; Li, F.; Xue, S.; Lin, H. L.; Sun, Y.; Cao, J.; Chen, S. F. Fe Doped Ni_3S_2 Nanosheet Arrays for Efficient and Stable Electrocatalytic Overall Urea Splitting. *ACS Appl. Energy Mater.* **2022**, *5*, 1183−1192.